

# Analysis of atmospheric neutrino oscillations in three-flavor neutrinos

T. Teshima<sup>1</sup> and T. Sakai

*Department of Applied Physics, Chubu University  
Kasugai 487-8501, Japan*

## Abstract

We analyze the atmospheric neutrino experiments of Super-Kamiokande (830-920 live days) using the three-flavor neutrino framework with the mass hierarchy  $m_1 \approx m_2 \ll m_3$ . We study the sub-GeV, multi-GeV neutrinos and upward through-going and stopping muons zenith angle distributions taking account of the Earth matter effects thoroughly. We obtain the allowed regions of mass and mixing parameters  $\Delta m_{23}^2$ ,  $\theta_{13}$  and  $\theta_{23}$ . In our present analysis, we used the solar neutrino small angle solution and large angle solution for  $\Delta m_{12}^2$  and  $\theta_{12}$ .  $\Delta m_{23}^2$  is restricted to 0.002-0.01 eV<sup>2</sup> and  $\theta_{13} < 13^\circ$ ,  $35^\circ < \theta_{23} < 55^\circ$  in 90% C.L. For  $\theta_{12}$ , there is no difference between the large angle solution and the small one. From  $\chi^2$  fit, the minimum  $\chi^2 = 55$  (54 DOF) is obtained at  $\Delta m_{23}^2 = 4 \times 10^{-3} \text{eV}^2$ ,  $\theta_{13} = 10^\circ$  and  $\theta_{23} = 45^\circ$ . In a two flavor mixing approximation ( $\theta_{13} = 0$ ), the minimum  $\chi^2 = 61$  (54 DOF) is obtained at  $\Delta m_{23}^2 = 3 \times 10^{-3} \text{eV}^2$  and  $\theta_{23} = 45^\circ$ . If  $\theta_{13} = 10^\circ$  is real, the detected  $\nu_e$  events in K2K experiment will be about 10 times as large as events expected in  $\theta_{13} = 0$  case .

PACS number(s): 12.15.Ff, 13.15.+g, 14.60.Pq

---

<sup>1</sup>E-mail: teshima@isc.chubu.ac.jp

# 1 INTRODUCTION

Super-Kamiokande collaboration has confirmed a neutrino oscillation by their atmospheric neutrino experiments [1]. In their two-flavor mixing analyses of the sub-GeV and the multi-GeV zenith angle distribution, it has been obtained that the  $\nu_\mu \leftrightarrow \nu_\tau$  oscillation is preferred to the  $\nu_\mu \leftrightarrow \nu_e$  oscillation and the range of mass parameter  $\Delta m^2$  is from  $10^{-3}\text{eV}^2$  to  $10^{-2}\text{eV}^2$ . Recently, Super-Kamiokande collaboration has reported that the  $\nu_\mu \leftrightarrow \nu_\tau$  oscillation is maximally  $\sin^2 2\theta = 0.9$ – $1$  and mass parameter  $\Delta m^2$  is from  $2.5 \times 10^{-3}\text{eV}^2$  to  $5 \times 10^{-3}\text{eV}^2$ , using the sub-GeV, multi-GeV neutrino and upward muons zenith angle distribution experiments (830–920 live days) [2].

However, these results are obtained from the two-flavor neutrino analyses. In order to account for the solar neutrino anomaly data together with atmospheric neutrino experiments, three flavor neutrinos are necessary at least. In three-flavor neutrinos scenario[3, 4] with a mass hierarchy  $m_1 \approx m_2 \ll m_3$ , there are necessary two mass parameters  $\Delta m_{12}^2$  and  $\Delta m_{23}^2$ , and three mixing angles  $\theta_{12}$ ,  $\theta_{13}$  and  $\theta_{23}$ . Solar neutrino anomaly gives constraint on only three parameters  $\Delta m_{12}^2$ ,  $\theta_{12}$  and  $\theta_{13}$ . The MSW solution for solar neutrinos predicts the large mixing angle solution ( $\Delta m_{12}^2 = 4 \times 10^{-6} - 7 \times 10^{-5}\text{eV}^2$ ,  $\sin^2 2\theta_{12} = 0.6$ – $0.9$ ) and the small mixing angle solution ( $\Delta m_{12}^2 = 3 \times 10^{-6}$ – $1.2 \times 10^{-5}\text{eV}^2$ ,  $\sin^2 2\theta_{12} = 0.003$ – $0.01$ ) for  $\theta_{13} = 0^\circ$ – $20^\circ$ , and these large and small mixing angle solutions are merged for  $25^\circ$ – $50^\circ$  [5]. The vacuum solution is also obtained as  $\Delta m_{12}^2 \sim 10^{-10}\text{eV}^2$ . However, CHOOZ experiment [6] which is a terrestrial experiment using reactor neutrinos gives a strong constraint  $\sin^2 2\theta_{13} < 0.18$  for large  $\Delta m_{23}^2$  and  $\Delta m_{23}^2 < 0.9 \times 10^{-3}\text{eV}^2$  for  $\sin^2 2\theta_{13} \sim 1$ . From the recent many atmospheric neutrino analyses [1, 2, 7, 4] using either two- or three-flavor neutrinos framework,  $\Delta m_{23}^2 = 10^{-3}$ – $10^{-2}\text{eV}^2$  is obtained. Therefore, it can be said that the mixing angle  $\theta_{13}$  is small but not necessarily 0.

In the three-flavor neutrino framework, if the mixing parameter  $\theta_{13}$  is not zero, it is necessary to consider the interplay between two mass parameters  $\Delta m_{12}^2$ ,  $\Delta m_{23}^2$  and three mixing angles  $\theta_{12}$ ,  $\theta_{13}$ ,  $\theta_{23}$  for atmospheric neutrino experimental analyses. The oscillation

term  $\sin^2 1.27 \frac{\Delta m_{12}^2}{E} L$  cannot be neglected though  $\Delta m_{12}^2 \ll \Delta m_{23}^2$ , because the term is not so small in the sub-GeV experiment ( $E = 0.2 \sim 1.3 \text{ GeV}$ ) of atmospheric neutrino with zenith angle  $\theta \sim 180^\circ$  at which  $L \sim 10000 \text{ km}$ . In the multi-GeV experiment ( $E > 1.3 \text{ GeV}$ ) of atmospheric neutrino and terrestrial short- and long-baseline experiments, the neutrino oscillation term  $\sin^2 1.27 \frac{\Delta m_{12}^2}{E} L$  can be neglected. The angle  $\theta_{13}$  has been seen to be small, then the  $\theta_{13}$  is approximated to be 0 in usual analyses. However, in the case considering the matter effects of the Earth, above approximation is not appropriate. The matter effect is expressed by the induced mass squared  $A = 2\sqrt{2}EG_F N_e = 7.59\rho E \times 10^{-5} \text{ eV}^2$ , where  $N_e$  is the number density of electrons,  $E$  is the energy of neutrinos (measured in GeV) and  $\rho$  is the matter density (measured in  $\text{gm/cm}^3$ ). The Earth density  $\rho$  is  $3.5 \sim 13 \text{ g/cm}^3$  and the multi-GeV experiment energy of neutrinos ranges from  $1.3 \text{ GeV}$  to  $100 \text{ GeV}$ . Then the value of  $A$  go through the value of mass parameter  $\Delta m_{23}^2$  and the MSW effect occurs in the mixing angle  $\theta_{13}$  (see section 3).

In this paper, we analyze the Super-Kamiokande atmospheric neutrino experimental data (850–920 live days) [2] of sub-GeV and multi-GeV neutrino, upward through-going and stopping muons, using the three-flavor neutrino framework with the hierarchy  $m_1 \approx m_2 \ll m_3$ . In previous paper [4], we analyzed the 535 live days data of Super-Kamiokande atmospheric neutrino experiment [1] using similar framework to the present analysis, approximating the Earth density to be constant. In this present analysis, we will pursue a full calculation adopting the varying density of the Earth. We will also discuss the long-baseline K2K experiment [8] in the three-flavor neutrino framework.

## 2 NEUTRINO OSCILLATION IN THREE-FLAVOR NEUTRINOS

The unitary matrix  $U$  which transforms the mass eigenstate neutrinos  $\nu_\alpha$  to the flavor eigenstate neutrinos  $\nu_l$  as the formula

$$\nu_l = \sum_{\alpha=1}^3 U_{l\alpha} \nu_\alpha, \quad l = e, \mu, \tau, \quad (1)$$

is parametrized as follows:

$$\begin{aligned}
U &= \exp(i\theta_{23}\lambda_7) \exp(i\theta_{13}\lambda_5) \exp(i\theta_{12}\lambda_2) \\
&= \begin{pmatrix} c_{12}c_{13} & s_{12}c_{13} & s_{13} \\ -s_{12}c_{23} - c_{12}s_{23}s_{13} & c_{12}c_{23} - s_{12}s_{23}s_{13} & s_{23}c_{13} \\ s_{12}s_{23} - c_{12}c_{23}s_{13} & -c_{12}s_{23} - s_{12}c_{23}s_{13} & c_{23}c_{13} \end{pmatrix}, \\
&\quad c_{ij} = \cos \theta_{ij}, \quad s_{ij} = \sin \theta_{ij}.
\end{aligned} \tag{2}$$

in a case disregarding the CP violation. We assume the mass hierarchy

$$m_1 \approx m_2 \ll m_3, \tag{3}$$

then  $\Delta m_{12}^2 \ll \Delta m_{13}^2 \simeq \Delta m_{23}^2$ . In this mass hierarchy, the transition probabilities  $P(\nu_l \rightarrow \nu_{l'})$  can be written as

$$P(\nu_l \rightarrow \nu_l) = 1 - 2(1 - 2U_{l3}^2 - U_{l1}^4 - U_{l2}^4 + U_{l3}^4)S_{12} - 4U_{l3}^2(1 - U_{l3}^2)S_{23}, \tag{4}$$

$$P(\nu_l \rightarrow \nu_{l'}) = P(\nu_{l'} \rightarrow \nu_l) = 2(U_{l1}^2 U_{l'1}^2 + U_{l2}^2 U_{l'2}^2 - U_{l3}^2 U_{l'3}^2)S_{12} + 4U_{l3}^2 U_{l'3}^2 S_{23}, \tag{5}$$

where  $S_{\alpha\beta}$  is a term representing the neutrino oscillation defined as;

$$S_{\alpha\beta} = \sin^2 1.27 \frac{\Delta m_{\alpha\beta}^2}{E} L. \tag{6}$$

Here  $\Delta m_{\alpha\beta}^2 = |m_\alpha^2 - m_\beta^2|$ ,  $E$  and  $L$  are measured in units  $\text{eV}^2$ ,  $\text{GeV}$  and  $\text{km}$ , respectively. For the mass parameter  $\Delta m_{12}^2$  and mixing angle  $\theta_{12}$ , we use values obtained in the solar neutrino experimental analyses[5]: the large mixing angle solution  $\Delta m_{12}^2 = 3 \times 10^{-5} \text{eV}^2$ ,  $\sin^2 2\theta_{12} = 0.7$ , and small mixing angle solution  $\Delta m_{12}^2 = 10^{-5} \text{eV}^2$ ,  $\sin^2 2\theta_{12} = 0.005$ . It should be noted that the oscillation term  $S_{12} = \sin^2 1.27 \frac{\Delta m_{12}^2}{E} L$  cannot be neglected in the sub-GeV experiment of atmospheric neutrino though  $\Delta m_{12}^2 \ll \Delta m_{23}^2$ , because this oscillation term is not so small in sub-GeV neutrino energy ( $E = 0.2\text{--}1.3 \text{GeV}$ ) with zenith angle  $\theta \sim 180^\circ$  ( $L \sim 10000 \text{km}$ ).

In the atmospheric neutrino experiments, the matters of the Earth have a important effect. Matter effect is represented by a term  $A = 2\sqrt{2}EG_F N_e = 7.59\rho E \times 10^{-5} \text{eV}^2$  induced by the Earth matter, where  $\rho$  is the matter density. In the Earth,  $\rho = 3.5 - 13 \text{g/cm}^3$ , and

sub-GeV and multi-GeV neutrino energy ranges from 0.1GeV to 100GeV, then the value of  $A$  goes through those of  $\Delta m_{12}^2$  and  $\Delta m_{23}^2$  and the resonance happens in mixing angles  $\theta_{12}$  and  $\theta_{13}$  as will be seen in Eqs.(8)–(11) and Eqs.(13)–(16). In the sub-GeV neutrino energy,  $A \sin 2\theta_{13}/2\Delta m_{23}^2 \ll 1$ , then we can approximate the mixing matrix  $U$  as [9]

$$U_{\text{sub}}^M = \exp(i\lambda_7\theta_{23}) \exp(i\lambda_5\theta_{13}) \exp(i\lambda_2\theta_{12}^M), \quad (7)$$

where

$$\sin 2\theta_{12}^M = \frac{\Delta m_{12}^2}{\Delta m_{12}^{M2}} \sin 2\theta_{12}, \quad (8)$$

$$\Delta m_{12}^{M2} = m_2^{M2} - m_1^{M2}, \quad \Sigma = m_1^2 + m_2^2, \quad (9)$$

$$m_{1,2}^{M2} = \frac{1}{2} \left\{ (\Sigma + A \cos^2 \theta_{13}) \mp \sqrt{(A \cos^2 \theta_{13} - \Delta m_{12}^2 \cos 2\theta_{12})^2 + (\Delta m_{12}^2 \sin 2\theta_{12})^2} \right\}, \quad (10)$$

$$m_3^{M2} = m_3^2 + A \sin^2 \theta_{13}. \quad (11)$$

On the other hand,  $A \sin 2\theta_{13}/2\Delta m_{23}^2$  is not so small in multi-GeV neutrino and upward muon energy. In this case, the mixing matrix can be expanded by powers of a quantity  $\Delta m_{12}^2 \sin 2\theta_{12}/2m_3^2$  which is very small. In the lowest order, the mixing matrix is expressed as

$$U_{\text{multi}}^M = \exp(i\lambda_7\theta_{23}) \exp(i\lambda_5\theta_{13}^M), \quad (12)$$

where

$$\sin 2\theta_{13}^M = \frac{\Delta m_{13}^2}{\Delta m_{13}^{M2}} \sin 2\theta_{13}, \quad (13)$$

$$\Delta m_{13}^{M2} = m_3^{M2} - m_1^{M2}, \quad \Lambda = \Sigma - \Delta m_{12}^2 \cos 2\theta_{12}, \quad \Sigma = m_1^2 + m_2^2, \quad (14)$$

$$m_{1,3}^{M2} = \frac{1}{2} \left\{ (m_3^2 + \frac{\Lambda}{2} + A) \mp \sqrt{(A - \Delta m_{13}^2 \cos 2\theta_{13})^2 + (\Delta m_{13}^2 \sin 2\theta_{13})^2} \right\}, \quad (15)$$

$$m_2^{M2} = \frac{1}{2} (\Sigma + \Delta m_{12}^2 \cos 2\theta_{12}). \quad (16)$$

These expressions correspond to the neutrino case, and  $A$  for the anti-neutrino case has an opposite sign of the neutrino case. From these expressions, we can recognize that

a resonance exists at  $A \approx \Delta m_{13}^2 \cos 2\theta_{13}$  of  $\sin 2\theta_{13}^M$ . When  $\Delta m_{13}^2 = 3 \times 10^{-3} \text{eV}^2$  and  $\cos 2\theta_{13} \sim 1$ , the resonance occurs at  $E \sim 10 \text{ GeV}$ .

When the density of the Earth matter is constant, the transition probability  $P^M(\nu_l \rightarrow \nu_{l'})$  with the matter effects can be expressed by the expression (5) with  $U$  and  $\Delta m_{\alpha\beta}^2$  replaced by  $U^M$  and  $\Delta m_{\alpha\beta}^{M2}$ . Actual density of the Earth is not constant but the density in shells which compose the Earth is almost constant. The net transition probability  $P_{\nu_l \rightarrow \nu_{l'}}$  of neutrinos going through the Earth can be given by connecting the transition amplitudes of each shell. The transition amplitude in  $k$ -th shell is expressed as

$$T_{l'l}(M_k, x_k) = \sum_{\alpha} (U^{M_k})_{l'\alpha} (U^{M_k*})_{l\alpha} \exp \left( -i \frac{m_{\alpha}^{M_k2}}{2p} x_k \right), \quad (17)$$

where  $U^{M_k}$  represents the mixing matrix containing the  $k$ -th shell matter effects,  $m_{\alpha}^{M_k}$  the mass of  $\nu_{\alpha}$  in the  $k$ -th shell and  $x$  the length traveling in the  $k$ -th shell. Using this transition amplitude, we get the transition probability as follows:

$$P_{\nu_l \rightarrow \nu_{l'}} = \left| \sum_{l_1, l_2, \dots} T_{l'l_{n-1}}(M_n, x_n) T_{l_{n-1}l_{n-2}}(M_{n-1}, x_{n-1}) \cdots \right. \\ \left. \cdots T_{l_2l_1}(M_2, x_2) T_{l_1l}(M_1, x_1) \right|^2. \quad (18)$$

Calculation using this expression is very complicated and cannot be carry out analytically, then we calculate this numerically.

### 3 NUMERICAL ANALYSES OF ATMOSPHERIC NEUTRINOS

In this work, we analyze the ratio  $N_{\text{Exp}}(l)/N_{\text{MC}}(l)$  of experimentally observed events  $N_{\text{Exp}}(l)$  and expected events  $N_{\text{MC}}(l)$  without oscillation, where  $l$  represents  $\mu$ -like and  $e$ -like events. The zenith angle  $\theta$  dependent events  $dN_{\text{Exp}}(l)/d \cos \theta$  and  $dN_{\text{MC}}(l)/d \cos \theta$  are defined as

$$\frac{dN_{\text{Exp}}(l)}{d \cos \theta} = \sum_{\nu_{l'}} \int \epsilon_l(E_l) \sigma_{\nu_l}(E_{\nu_{l'}}, E_l, \psi) F_{\nu_{l'}}(E_{\nu_{l'}}, \theta - \psi) P^M(\nu_{l'} \rightarrow \nu_l) dE_{\nu_{l'}} dE_l d \cos \psi, \quad (19)$$

$$\frac{dN_{\text{MC}}(l)}{d \cos \theta} = \int \epsilon_l(E_l) \sigma_{\nu_l}(E_{\nu_l}, E_l, \psi) F_{\nu_l}(E_{\nu_l}, \theta - \psi) dE_{\nu_l} dE_l d \cos \psi, \quad (20)$$

where the summation  $\sum_{\nu_{l'}}$  are taken over  $\nu_\mu$  and  $\nu_e$ . In these expressions, processes of  $\bar{\nu}_\mu$  and  $\bar{\nu}_e$  are contained.  $\epsilon_l(E_l)$  is the detection efficiency of the detector for  $l$ -type charged lepton with energy  $E_l$ .  $\sigma_{\nu_l}(E_{\nu_{l'}}, E_l, \psi)$  is the differential cross section of scattering  $l$  with energy  $E_l$  by incident  $\nu_l$  with energy  $E_{\nu_{l'}} = E_{\nu_l}$ , where angle  $\psi$  is the scattering angle between the directions of incident  $\nu_l$  and scattered  $l$ .  $F_{\nu_{l'}}(E_{\nu_{l'}}, \theta)$  is the incident  $\nu_{l'}$  flux with energy  $E_{\nu_{l'}}$  produced at the atmosphere coming to the detector with zenith angle  $\theta$ .  $E_{\nu_l}$  and  $\theta$  dependences of  $F_{\nu_l}(E_{\nu_l}, \theta)$  for multi-GeV experiment ( $E_{\nu_l} > 1.33\text{GeV}$ ) are given in Refs. [10, 11]. These dependences including the geomagnetic effects for sub-GeV case ( $0.2\text{GeV} < E_{\nu_l} < 1.33\text{GeV}$ ) are taken from Ref. [12]. Other informations of  $\epsilon_l(E_l)$  and  $\sigma_{\nu_l}(E_{\nu_l}, E_l, \psi)$  are given in Ref. [13]. The upward through-going muons (thru-muons) and stopping muons (stop-muons) fluxes are shown in Ref. [13]. Typical energies of  $\nu_\mu$  that produce thru- and stop-muons are 100GeV and 10GeV, respectively. Explicit calculation of Eqs. (19) and (20) is explained precisely in Appendix A of the second paper in Ref. [4].

$P^M(\nu_{l'} \rightarrow \nu_l)$  is the transition probability with the matter effects expressed in Eq. (18). The Earth consists of 5 shells approximately [14]; the density of the most outside shell (radius  $r = 5991 - 6371\text{km}$ ) is  $3.5\text{g/cm}^3$ , the next outside shell ( $r = 5719 - 5991\text{km}$ )  $4\text{g/cm}^3$ , the middle shell ( $r = 3519 - 5719\text{km}$ )  $5\text{g/cm}^3$ , the outer core shell ( $r = 1231 - 3519\text{km}$ )  $11\text{g/cm}^3$ , the inner core ( $r = 0 - 1231\text{km}$ )  $13\text{g/cm}^3$ . A number of the shells through which neutrinos pass changes with a change of the zenith angle  $\theta$ . For example, the number of the shell is 0 for  $0 < \theta < 90^\circ$  and 9 for  $\theta = 180^\circ$ .

The zenith angle distributions of sub-GeV, multi-GeV neutrino events and upward thru- and stop-muons fluxes are given by the SuperKamiokande 850-920 live days experiments [2]. The data are tabulated in Table I. These values are taken from the experimental event data and Monte-Carlo simulations which are given graphically in Ref. [2].  $\mu$ -like events include the fully contained and partially contained events. Errors represent statistical ones only.

Since  $P^M(\nu_{l'} \rightarrow \nu_l)$  is a function of  $\Delta m_{12}^2, \Delta m_{23}^2, \theta_{12}, \theta_{13}$  and  $\theta_{23}$ , the ratio  $(dN_{\text{Exp}}(l))$

Table 1:  $e$ -like,  $\mu$ -like atmospheric neutrino data, and upward muons fluxes of SuperKamiokande experiments (850-920 live days data). These values are the ratios of experimental data and Monte-Carlo simulations which are obtained from the graphs in Ref. [2].  $\mu$ -like events include fully contained and partially contained events, and errors represent statistical ones only.

Sub-GeV data		
$\cos\theta$ range	$e$ -like event ratio $N_{\text{Exp}}/N_{\text{MC}}$	$\mu$ -like event ratio $N_{\text{Exp}}/N_{\text{MC}}$
$-1.0-0.8$	$1.10 \pm 0.08$	$0.66 \pm 0.05$
$-0.8-0.6$	$1.10 \pm 0.08$	$0.52 \pm 0.05$
$-0.6-0.4$	$1.05 \pm 0.08$	$0.59 \pm 0.05$
$-0.4-0.2$	$0.98 \pm 0.08$	$0.67 \pm 0.05$
$-0.2-0.0$	$0.99 \pm 0.08$	$0.64 \pm 0.05$
$0.0-0.2$	$1.10 \pm 0.08$	$0.71 \pm 0.05$
$0.2-0.4$	$1.09 \pm 0.08$	$0.80 \pm 0.06$
$0.4-0.6$	$0.90 \pm 0.07$	$0.82 \pm 0.06$
$0.6-0.8$	$1.15 \pm 0.08$	$0.80 \pm 0.06$
$0.8-1.0$	$0.94 \pm 0.07$	$0.87 \pm 0.06$

Multi-GeV data		
$\cos\theta$ range	$e$ -like event ratio $N_{\text{Exp}}/N_{\text{MC}}$	$\mu$ -like event ratio $N_{\text{Exp}}/N_{\text{MC}}$
$-1.0-0.8$	$0.83 \pm 0.18$	$0.47 \pm 0.07$
$-0.8-0.6$	$1.19 \pm 0.18$	$0.51 \pm 0.07$
$-0.6-0.4$	$0.97 \pm 0.15$	$0.45 \pm 0.06$
$-0.4-0.2$	$1.18 \pm 0.16$	$0.55 \pm 0.07$
$-0.2-0.0$	$1.04 \pm 0.14$	$0.63 \pm 0.07$
$0.0-0.2$	$0.94 \pm 0.13$	$0.81 \pm 0.08$
$0.2-0.4$	$1.33 \pm 0.16$	$0.91 \pm 0.09$
$0.4-0.6$	$0.85 \pm 0.15$	$0.99 \pm 0.10$
$0.6-0.8$	$1.00 \pm 0.17$	$0.85 \pm 0.09$
$0.8-1.0$	$1.27 \pm 0.21$	$1.00 \pm 0.10$

Upward through-going $\mu$ data	
$\cos\theta$ range	$\mu$ flux ratio $N_{\text{Exp}}/N_{\text{MC}}$
$-1.0-0.9$	$0.84 \pm 0.11$
$-0.9-0.8$	$0.90 \pm 0.11$
$-0.8-0.7$	$0.72 \pm 0.09$
$-0.7-0.6$	$0.95 \pm 0.10$
$-0.6-0.5$	$0.86 \pm 0.09$
$-0.5-0.4$	$0.76 \pm 0.08$
$-0.4-0.3$	$0.82 \pm 0.09$
$-0.3-0.2$	$1.09 \pm 0.09$
$-0.2-0.1$	$0.96 \pm 0.08$
$-0.1-0.0$	$1.14 \pm 0.08$

Upward stopping $\mu$ data	
$\cos\theta$ range	$\mu$ flux ratio $N_{\text{Exp}}/N_{\text{MC}}$
$-1.0-0.8$	$0.55 \pm 0.10$
$-0.8-0.6$	$0.50 \pm 0.09$
$-0.6-0.4$	$0.60 \pm 0.09$
$-0.4-0.2$	$0.47 \pm 0.08$
$-0.2-0.0$	$0.75 \pm 0.10$



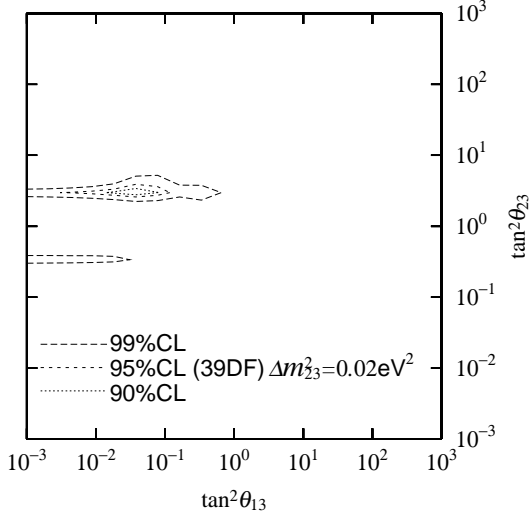
$/d \cos \theta)/(dN_{\text{MC}}(l)/d \cos \theta)$  of the zenith angle distributions is a function of  $\Delta m_{12}^2, \Delta m_{23}^2, \theta_{12}, \theta_{13}, \theta_{23}$  and  $\theta$ . We analyze the atmospheric neutrino data fixing the values of parameters  $\Delta m_{12}^2$  and  $\sin^2 2\theta_{12}$  determined from the solar neutrino experiments [5] as  $\Delta m_{12}^2 = 3 \times 10^{-5} \text{eV}^2$  and  $\sin^2 2\theta_{12} = 0.7$ , which corresponds to the large angle solution, and  $\Delta m_{12}^2 = 10^{-5} \text{eV}^2$  and  $\sin^2 2\theta_{12} = 0.005$ , which corresponds to the small angle solution. We treat the ratios of the zenith angle distributions of the experimental events and the ones of Monte-Carlo simulation,  $(N_{\text{Exp}}(l)/N_{\text{MC}}(l))_i$ , where  $i$  represents the region number of the bins of zenith angle  $\theta$ .

We calculate numerically the  $\chi^2$  defined as

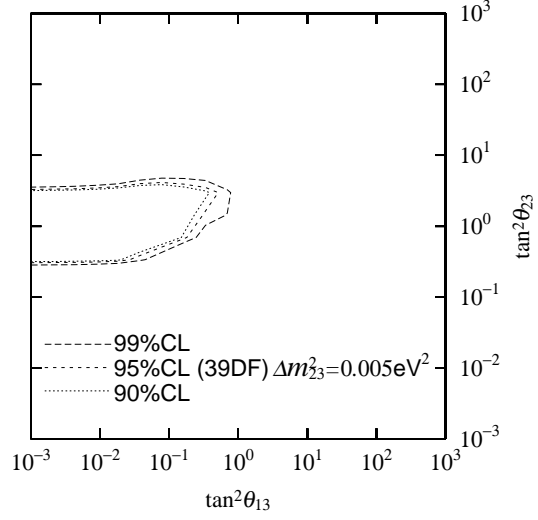
$$\chi^2 = \sum_{i, l} \frac{\left\{ (N_{\text{Exp}}(l)/N_{\text{MC}}(l))_i^{\text{cal}} - (N_{\text{Exp}}(l)/N_{\text{MC}}(l))_i^{\text{data}} \right\}^2}{(\sigma_{\text{st}})_i^2 + (\sigma_{\text{sy}})_i^2}. \quad (21)$$

For the sub-GeV, multi-GeV and upward thru-muon experiments, the summation on  $i$  are from 1 to 10 of zenith angle range bins and for the upward stop-muon, from 1 to 5. The summation on  $l$  are over  $\mu$  and  $e$  for the sub-GeV and multi-GeV experiments.  $\sigma_{\text{st}}$  represents the statistical error and  $\sigma_{\text{sy}}$  systematic one. We assumed that the value of  $\sigma_{\text{sy}}$  is 5% of an amount of the  $N_{\text{MC}}$  for the sub-GeV and multi-GeV neutrino data, 10% for the upward stop-muon data and 20% for the upward thru-muon data. We adopted the rather large value of  $\sigma_{\text{sy}}$  for upward thru-muons, because there exists larger uncertainty of neutrino flux for high energy neutrinos. We estimated the values of  $\chi^2$  for the various values of  $\Delta m_{23}^2, \theta_{13}$  and  $\theta_{23}$ .

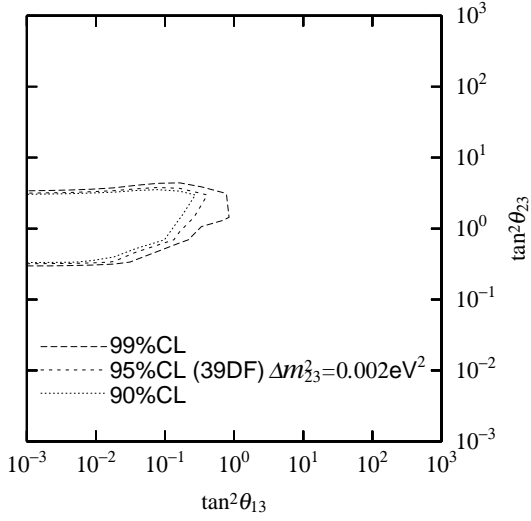
In Fig. 1, we showed the contour plots of  $\chi^2$  in the  $\tan^2 \theta_{13}$ – $\tan^2 \theta_{23}$  plane for various values of  $\Delta m_{23}^2$ . These plots show the  $\chi^2$  of the sub-GeV neutrino plus multi-GeV neutrino zenith angle distributions for the large  $\theta_{12}$  angle solution. We did not show the plots for the small angle solution, because  $\chi^2$  for the small angle solution is almost similar to that for large one. In these figures, broken thick, broken thin and dotted curves denote the regions allowed in 99%, 95% and 90% C.L., respectively. From these plots we can say that the values of allowed  $\Delta m_{23}^2$  is from  $2 \times 10^{-3} \text{eV}^2$  to  $10^{-2} \text{eV}^2$ ,  $\theta_{13}$  is  $< 17^\circ$  and  $\theta_{23}$  is from  $35^\circ$  to  $55^\circ$ .



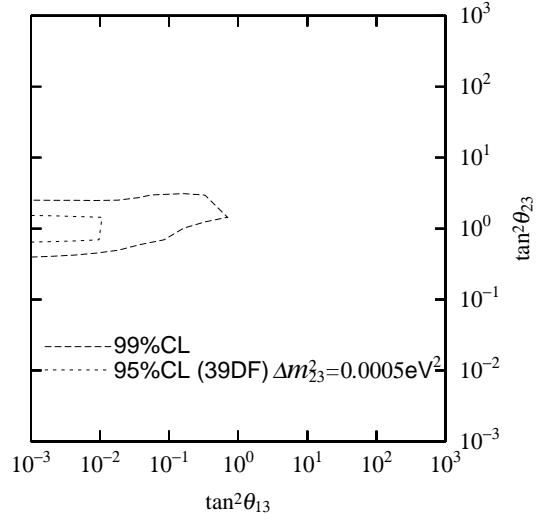
(a)



(b)

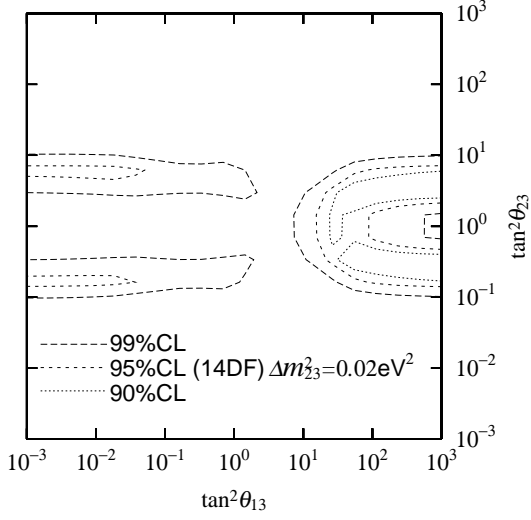


(c)

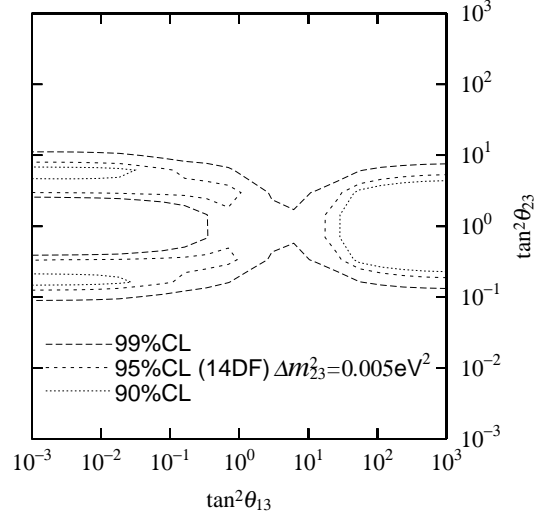


(d)

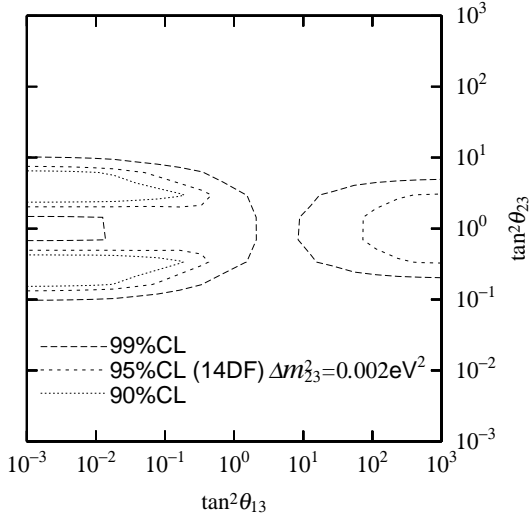
Figure 1: The plots of allowed regions in the  $\tan^2 \theta_{13}$ – $\tan^2 \theta_{23}$  plane determined by the sub-GeV neutrino plus multi-GeV neutrino zenith angle distributions of SuperKamiokande 848 live days data. These figures correspond to the large  $\theta_{12}$  angle solution,  $\Delta m^2_{12} = 3 \times 10^{-5} \text{eV}^2$  and  $\sin^2 2\theta = 0.7$ . In these figures, broken thick, broken thin and dotted curves denote the regions allowed in 99%, 95% and 90% C.L., respectively.



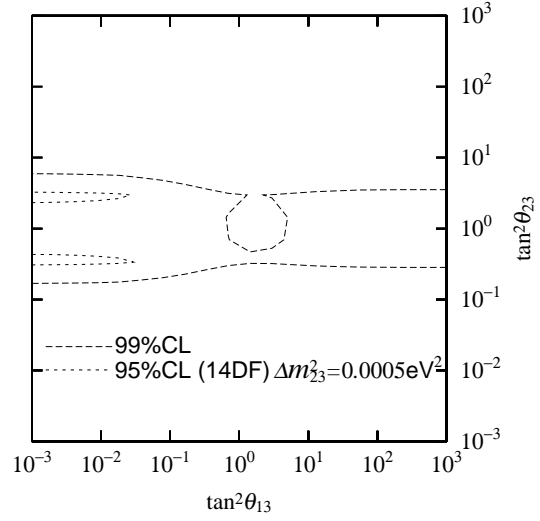
(a)



(b)

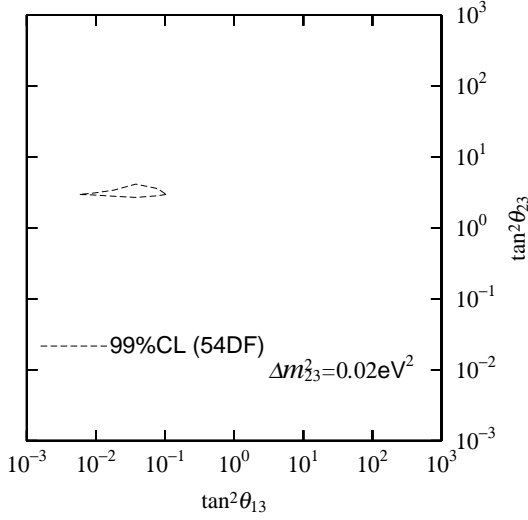


(c)

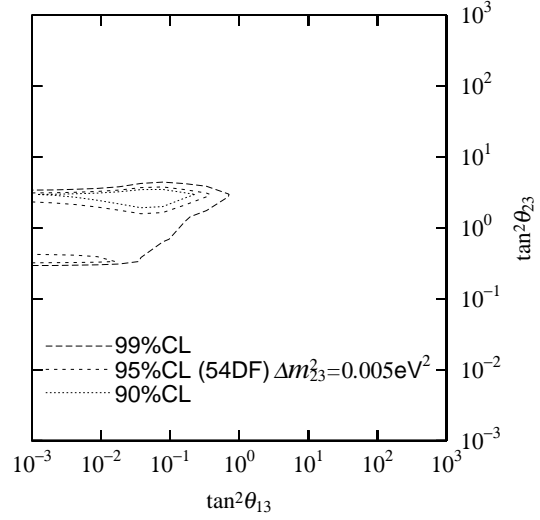


(d)

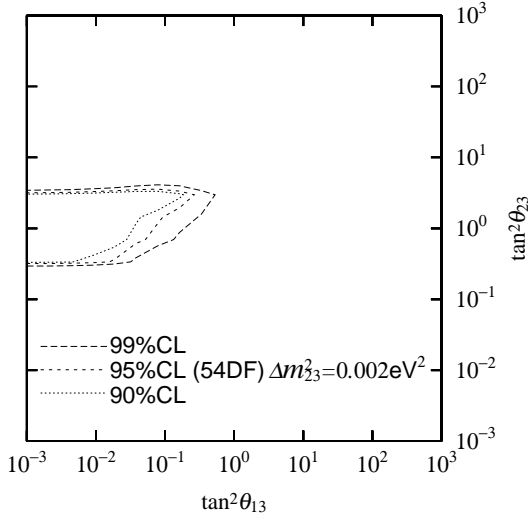
Figure 2: The plots of allowed regions in  $\tan^2 \theta_{13}$ – $\tan^2 \theta_{23}$  plane determined by the combination of the zenith angle distributions of the upward thru- and stop-muon SuperKamiokande 902-923 live days data for large  $\theta_{12}$  angle solution. There is no difference between the large  $\theta_{12}$  angle solution and small one. In these figures, broken thick, broken thin and dotted curves denote the regions allowed in 99%, 95% and 90% C.L., respectively.



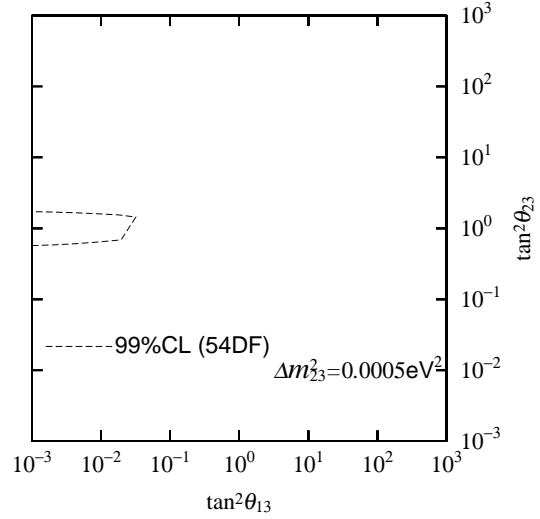
(a)



(b)



(c)



(d)

Figure 3: The plots of the allowed regions in  $\tan^2 \theta_{13}$ –  $\tan^2 \theta_{23}$  plane determined by the combination of the zenith angle distributions of the sub- and multi-GeV neutrinos and upward thru- and stop-muon data for large  $\theta_{12}$  angle solution. There is no difference between the large  $\theta_{12}$  angle solution and small one. In these figures, the broken thick, broken thin and dotted curves denote the regions allowed in 99%, 95% and 90% C.L., respectively.

Plots of the upward thru- plus stop-muons are shown in Fig. 2 for the large  $\theta_{12}$  angle solution. We did not show the plots for small angle solution, because there is no difference between the large  $\theta_{12}$  angle solution and small one. In these figures, sharp allowed regions similar to those of previous sub-GeV plus multi-GeV neutrinos data is not appeared. The reason is as follows: although stop-muons data show the sharp allowed regions similar to those of sub-GeV plus multi-GeV neutrino data, thru-muons data show the excluded regions near  $45^\circ$  of  $\theta_{23}$ . The latter situation is caused from small deficit (about 0.2) from 1 of the  $\mu$  event ratio  $N_{\text{Exp}}/N_{\text{MC}}$  as shown in Table 1.

In Fig. 3, we showed the contour plots of  $\chi^2$  for the combination of the sub-GeV and multi-GeV neutrinos, the upward thru- and stop-muons zenith angle distributions for large  $\theta_{12}$  solution. In these figures, broken thick, broken thin and dotted curves denote the regions allowed in 99%, 95% and 90% C.L., respectively.

From these plots, we can get the following results for the neutrino mass and mixing parameters:

- (1) As shown in Fig. 1, the allowed region for  $\Delta m_{23}^2$  obtained from the sub-GeV and multi-GeV neutrino experiments is from  $2 \times 10^{-3} \text{eV}^2$  to  $10^{-2} \text{eV}^2$  at 90% C.L., and the allowed region for  $\theta_{23}$  angle is from  $35^\circ$  to  $55^\circ$  and for  $\theta_{13}$  angle is less than  $17^\circ$ . The minimum  $\chi^2$  is obtained as 29 for 39 degrees of freedom (DOF) at  $\Delta m_{23}^2 = 5 \times 10^{-3} \text{eV}^2$ ,  $\theta_{13} = 10^\circ$  and  $\theta_{23} = 45^\circ$ . The minimum  $\chi^2$  in the restriction  $\theta_{13} = 0$  which corresponds to the two flavor mixing  $\nu_\mu - \nu_\tau$  approximation, is 30 for 39 DOF at  $\Delta m_{23}^2 = 4 \times 10^{-3} \text{eV}^2$ .
- (2) As shown in Fig. 2, the allowed region for  $\theta_{13}$  and  $\theta_{23}$  is excluded at small  $\theta_{13}$  and the maximal mixing of  $\theta_{23}$  for large values of  $\Delta m_{23}^2$ . This is because of the fact that the data in upward thru-muons has not so large deficit from the no-oscillation case as seen in the Table 1.
- (3) There is no significant difference between the large  $\theta_{12}$  solution and the small solution. This fact is not seen from these figures, but we can see from our numerical calculation that the difference between the large angle solution and the small one is less than 1% for

multi-GeV neutrinos and upward muons and less than 10 % for sub-GeV neutrinos.

(4) The allowed region for  $\Delta m_{23}^2$  obtained from the sub- and multi-GeV neutrinos, and upward thru- and stop-muons is given as  $2 \times 10^{-3} \text{eV}^2$  to  $\times 10^{-2} \text{eV}^2$ , and for  $\theta_{23}$  as  $35^\circ$  to  $55^\circ$  and for  $\theta_{13}$  as less than  $13^\circ$ . The minimum  $\chi^2$  is obtained as 55 for 54 DOF at  $\Delta m_{23}^2 = 4 \times 10^{-3} \text{eV}^2$ ,  $\theta_{13} = 10^\circ$  and  $\theta_{23} = 45^\circ$ . The minimum  $\chi^2$  in the restriction  $\theta_{13} = 0^\circ$  which corresponds to the two flavor mixing  $\nu_\mu - \nu_\tau$  approximation, is 61 for 54 DOF at  $\Delta m_{23}^2 = 3 \times 10^{-3} \text{eV}^2$  and  $\theta_{23} = 45^\circ$ . These results are the same as the result obtained by Super-Kamiokande collaboration [2].

(5) It is interesting that the minimum of  $\chi^2$  is obtained at not  $\theta_{13} = 0$  but  $\theta_{13} = 10^\circ$ , though the difference between  $\chi^2$  for  $\theta_{13} = 0$  case and that for  $\theta_{13} = 10^\circ$  case is not so large. This result is consistent with the CHOOZ experiment [6]. The CHOOZE experiment predicts the results:  $\theta_{13} < 13^\circ$  for  $\Delta m_{23}^2 = 3 \times 10^{-3} \text{eV}^2$ .

We will now discuss about the interesting feature that the mixing angle  $\theta_{13}$  is preferred to be about  $10^\circ$ . If this feature is real, the detected  $\nu_e$  events in the long baseline K2K experiment [8] will be about 10 times as large as the events expected in  $\theta_{13} = 0$  case. This is caused from the fact that the  $\nu_\mu$  flux produced at KEK is about 100 times as large as  $\nu_e$  flux and the transition probability is  $P(\nu_\mu \rightarrow \nu_e) \sim \sin^2 2\theta_{13} \sin^2 1.27 \Delta m_{23}^2 L/E$ ,  $E \sim 1.4 \text{GeV}$  and  $L = 250 \text{km}$ .

## 4 Conclusion

We analyzed the atmospheric neutrino experimental data of Super-Kamiokande [1] in the three-flavor neutrino framework with the mass hierarchy  $m_1 \approx m_2 \ll m_3$  and obtained the allowed regions of parameters  $\Delta m_{23}^2$ ,  $\theta_{13}$  and  $\theta_{23}$ , including the Earth matter effects thoroughly. We studied the event ratios of the sub- and multi-GeV, and upward thru- and stop-muons zenith angle distributions. From these atmospheric experiments, we can get the allowed region of mass parameter  $\Delta m_{23}^2$  restricted as  $0.002 \text{eV}^2$ – $0.01 \text{eV}^2$ , and mixing parameter  $\theta_{13}$  as less than  $13^\circ$  and  $\theta_{23}$  as  $35^\circ$ – $55^\circ$ . The value of  $\Delta m_{23}^2$  at the minimum

$\chi^2 = 55$  for 54 DOF is obtained as  $4 \times 10^{-3} \text{eV}^2$  at  $\theta_{13} = 10^\circ$  and  $\theta_{23} = 45^\circ$ . The minimum  $\chi^2 = 61$  for 54 DOF is obtained with the restriction  $\theta_{13} = 0$  at the  $\Delta m_{23}^2 = 3 \times 10^{-3} \text{eV}^2$  and  $\theta_{23} = 45^\circ$ . This fact seems very interesting for us because the mixing parameter  $\theta_{13}$  may not be 0. For mixing parameter  $\theta_{12}$ , the difference between the large angle solution and the small one is less than 1%. If  $\theta_{13}$  is about  $10^\circ$ , the detected  $\nu_e$  events in K2K experiment is about 10 times as large as events expected in  $\theta_{13} = 0$  case.

## References

- [1] T. Kajita (Super-Kamiokande Collaboration), in Proceedings of Neutrino'98, 18th International Conference on Neutrino Physics and Astrophysics, Takayama, Japan, June 4-9, 1998.
- [2] Y. Totsuka (Super-Kamiokande Collaboration), in Proceedings of XVth Particles and Nuclei International conference, PANIC99, Uppsala, June 10-19, 1999.
- [3] C. Y. Cardall and G. M. Fuller, Phys. Rev. **D 53**, 4421(1996); G. L. Fogli, E. Lisi, D. Montanio and G. Sciscia, Phys. Rev. **D 56**, 4365(1997); C. Meier and T. Ohlsson, hep-ph/9910270.
- [4] T. Teshima and T. Sakai, Prog. Theor. Phys. **101**, 147(1999); T. Sakai and T. Teshima, Prog. Theor. Phys. **102**, 629(1999).
- [5] G. L. Fogli, E. Lisi and D. Montanino, Phys. Rev. **D54**, 2048(1996); T. Teshima, T. Sakai and O. Inagaki, Int. J. Mod. Phys. **A14**, 1953(1999).
- [6] CHOOZ Collaboration: M. Apollonio *et al.*, Phys. Lett. **B420**, 397(1998).
- [7] G. L. Fogli, E. Lisi, A. Marrone, and G. Sciscia, Phys. Rev. **D59**, 033001(1998).
- [8] Y. Oyama(K2K Collaboration), talk at the YITP workshop on flavor physics, Kyoto, Japan, January, 1998. hep-ex/9803014.

- [9] T. Kuo and J. Pantaleone, Rev. Mod. Phys. **61**, 937(1989).
- [10] T. K. Gaisser, T. Stanev and G. Barr, Phys. Rev. **D38**, 85(1988).
- [11] M. Honda et al., Phys. Rev. **D52**, 4985(1995).
- [12] M. Honda *et al.*, private communication.
- [13] T. Kajita, *Physics and Astrophysics of Neutrinos*, edited by M. Fukugita and A. Suzuki, (Springer-Verlag, Tokyo, 1994).
- [14] E. D. Carlson, Phys. Rev. **D34**, 1453(1986).